Applied Catalysis B: Environmental 165 (2015) 547–554

Contents lists available at ScienceDirect

Applied Catalysis B: Environmental

journal homepage: www.elsevier.com/locate/apcatb

Sustainable production of aromatics from bio-oils through combined catalytic upgrading with *in situ* generated hydrogen

Fengbo Li[a,*], Yin Yuan[b,a], Zhijun Huang[a], Bingfeng Chen[a], Fosong Wang[a,**]

[a] *Beijing National Laboratory of Molecular Science, Key Laboratory of Green Printing, Institute of Chemistry, Chinese Academy of Sciences, Beijing 100190, P.R. China*

[b] *University of Chinese Academy of Sciences, Beijing, 100049, P. R. China*

ARTICLE INFO

Article history:
Received 5 August 2014
Received in revised form 16 October 2014
Accepted 20 October 2014
Available online 28 October 2014

Keywords:
Sustainable chemistry
Renewables
Catalytic upgrading
Bio-oils
Aromatics.

ABSTRACT

Pyrolysis liquids or bio-oils from rice husks are selectively converted into aromatics through a combined catalytic process, which includes two sequent steps: reforming and upgrading. Hydrogen from methanol and low-weight molecules in bio-oil is *in situ* generated in the reforming reactor. Methanol (16 wt% of total bio-oils) is added not only as the hydrogen donor, but also as polar solvent for homogenizing bio-oil and reducing its viscosity. Structured nickel nets are used as both the reforming catalyst and heating grid for gasifying high-boiling-point components of bio-oil. In the upgrading reactor, the combination of Co–Ru–Zr/silica with Pt-ZSM-5 gives the highest yield of aromatics (53.7%) and the lowest coke deposition (7.1%). Hydrogen for deoxygenation is generated from reforming of added methanol and low-weight molecules in bio-oil. Coke formation during fixed-bed upgrading can be significantly suppressed through the combined catalytic process.

1. Introduction

Pyrolysis liquids or bio-oils are carbon-rich liquids produced from fast pyrolysis of lignocellulosic biomass [1]. There are three thermal processes for converting biomass into more useful energy forms—pyrolysis, gasification and combustion [2]. Fast pyrolysis is the only process to give high yield of liquids (up to 75 wt%), which are considered as inexpensive renewable feedstocks for liquid fuel and chemicals [3]. However, there are several fundamental challenges of converting bio-oil into transport fuels and value-added chemicals. Firstly, bio-oils are low-quality fuels with high oxygen content of up to 60 wt% and immiscible with conventional hydrocarbon fuels. They cannot be directly used in gasoline and diesel engines. Secondly, bio-oils are acidic and unstable mixtures that have a water content of around 30 wt%. Polymerization and phase separation take place during storage. Thirdly, the complexity of biomass feedstocks and conversion processes results in lack of detailed models of describing physicochemical properties of bio-oil [4]. Despite these drawbacks, it is feasible to upgrade bio-oil to hydrocarbon fuels and chemicals through deoxygenation and zeolite cracking over well-designed catalysts [5–7].

There are three main methods for upgrading bio-oils—physical treatment, catalytic upgrading and chemical conversion [8]. Physical treatments include filtration to remove char microparticles, solvent addition to reduce the viscosity and emulsion to improve the miscibility with hydrocarbon fuels [9,10]. Catalytic upgrading of bio-oils is the most efficient way. Catalytic cracking and hydrotreating can deoxygenate bio-oils and give hydrocarbon mixtures with properties close to conventional transport fuels [11–17]. Oxygen of bio-oil can be reduced by zeolite cracking [18–21]. Catalytic reforming of bio-oils in vapor or liquid phases produces clean gaseous energy forms—hydrogen and syngas [22]. Chemical conversions, such as esterification and reactive distillation, are less common methods for upgrading bio-oils because of their high cost and relatively low efficiency [23–25]. The rapidly emerging research in improving bio-oil properties may increase its potential for biofuel and chemical production. However, the upgrading efficiency is relatively low and most of the research is performed over model compounds and catalysts only for fundamental purposes. Actually, more sophisticated catalytic systems are required to be developed from a practical angle to prove the feasibility and reliability of bio-oil upgrading.

Integrated catalytic upgrading processes can be divided into two types: catalytic pyrolysis to improve the quality of bio-oil and integrating different catalytic models in bio-oil upgrading process. Regalbuto [26] recently gave a perspective about several routes developed to directly convert biomass into hydrocarbon.

* Corresponding author. Tel.: +86 10 62634920; fax: +86 10 62559373.
** Corresponding author.
E-mail addresses: lifb@iccas.ac.cn (F. Li), fswang@iccas.ac.cn (F. Wang).

http://dx.doi.org/10.1016/j.apcatb.2014.10.050
0926-3373/

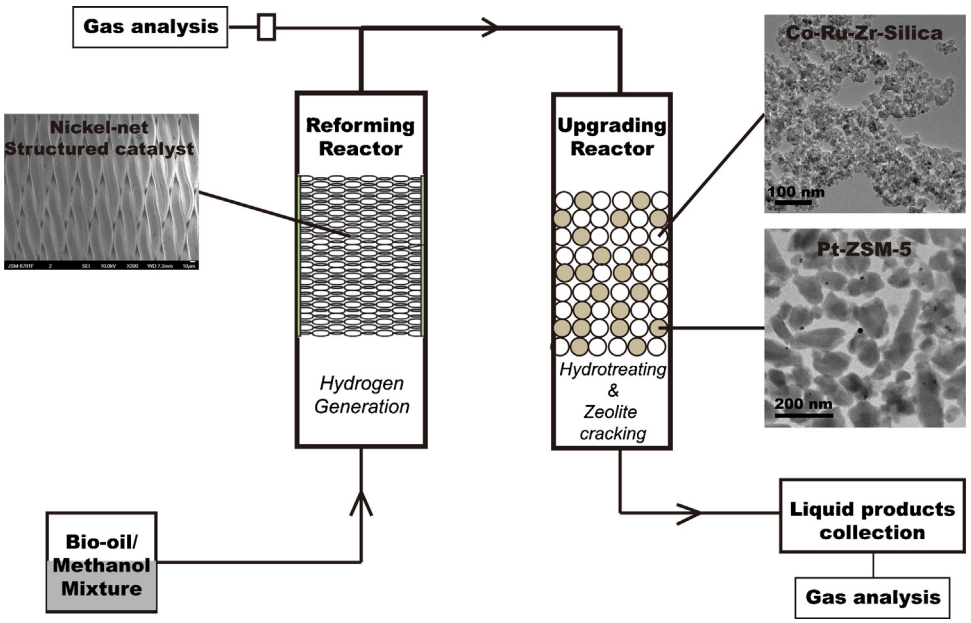

Scheme 1. Schematic illustration of the proposed combined catalytic upgrading of rice husks' pyrolysis oils.

However, there are several inherent problems in the catalytic pyrolysis—coking, catalyst regeneration and the reactor design for efficient mass and heat transfer. Vispute et al. [27] recently reported a breakthrough in converting bio-oils into aromatics and olefins with the carbon yield above 60% using an integrated catalytic approach that combines hydroprocessing with zeolite catalysis. Bio-oils are first incompletely deoxygenated with hydrogen at a moderate temperature and further processed over a zeolite catalyst in a fluidized bed reactor to produce aromatics and olefins. As pointed out by the authors, the integrated catalytic approach avoids the use of the large amount of expensive hydrogen and heavy coke deposition over the catalysts.

In this work, a well-designed integrated catalytic process is established for improving the quality of bio-oils. Bio-oils used in our research are manufactured from rice husks in a 100 ton/day pilot plant of YMB New Energy Co. (Jilin, China) (Fig. S1). The process includes two sequent steps in separate reactors: a reforming reactor and an upgrading reactor (as shown in Scheme 1). The function of reforming reactor is *in situ* generation of hydrogen from added hydrogen donors and low-weight molecules in bio-oil and no exterior hydrogen is introduced into the system. Methanol is not only the added hydrogen donor, but also polar solvent for homogenizing bio-oil and reducing its viscosity. The upgrading step combines hydrotreating catalysts and zeolite catalysts in one single reactor. Coke formation during fixed-bed upgrading can be significantly suppressed through the combined catalytic process. Two types of catalysts are packed in the reactor through a physical-mixture model. The mixture from the reforming reactor is directly led into the upgrading reactor to produce aromatic-enriched liquids.

Bio-oil of rice husk has a high oxygen content of approximately 50 wt%, which gives bio-oil a low energy density. Oxygen-containing compounds such as organic acids and other active molecules contribute to corrosiveness, phase separation and polymerization of bio-oil. The economic removal of oxygen from bio-oil is crucial to its successful application as an alternative to petroleum-derived hydrocarbon feedstocks and fuels. Oxygen can be rejected as water through hydrotreating with pure hydrogen or as carbon dioxide through zeolite cracking. The high oxygen content of bio-oil requires a large amount of hydrogen to achieve complete hydrodeoxygenation. Active molecules in bio-oil are prone to thermal polymerization and heavy coke deposition during zeolite cracking causes sharp degradation of the catalyst. Hydrogenation of these active compounds to alcohols can markedly suppress coke formation over zeolite catalysts [27].

Hydrogen is a tight and expensive resource. In the present industrial system, it is produced through costly and energy-intensive processes. The most commonly used route is SMR (steam-methane-reforming)–WGS (water-gas-shift)–PSA (pressure-swing-adsorption) [28]. A huge amount of CO_2 is released with hydrogen production from fossil feedstocks and fuels for generation of energy to drive the process. In China, coal is the main feedstock for steam reforming, which outlet sulfur and nitrogen oxide pollutants to the atmosphere. When considering environmental and economic cost of hydrogen production, sustainability of hydrogen-intensive conversion of bio-oil to hydrocarbons is doubtful. In this work, hydrogen for upgrading is generated from added methanol and light-weight organics of bio-oil. Bio-oils have been widely considered as renewable feedstocks for hydrogen production through catalytic reforming [7,22,29,30]. Water-soluble, small molecules are relatively easy to be reformed and partially supply hydrogen for further upgrading. Methanol is used as added hydrogen donor, which is safer and cheaper than pure hydrogen. Another advantage is that the addition of methanol homogenizes bio-oil and reduces its viscosity. This makes the injection proceed smoothly. Nickel catalysts have been extensively investigated as reforming catalysts for methanol and oxygenates reforming [31–34].

2. Experimental

2.1. Feedstock: bio-oil properties

Bio-oils (YMB-BO) used in our research were produced from rice husks in a 100 ton/day pilot plant of YMB New Energy Co. (Jilin, China) (Fig. S1). Fine char particles in the crude bio-oil were removed through a high-speed centrifuge. Basic properties of bio-oil were listed in Table 1 and its detailed chemical compositions were provided in Table S1. A well-calculated amount of methanol (16 wt%) was added into bio-oil to homogenize the mixture and

Table 1
Properties of YMB bio-oils.

Liquid\Properties	H_2O (wt%)	pH	Density (kg/m^3)	Viscosity (mm^2/s)	Solid (wt%)	LHV (mJ/kg)	Elemental compositions (wt%)				
							C	H	O	N	S
YMB Bio-oils	31	3.1	1.12	14.8	0.15	17.7	44.2	6.1	49.4	0.3	–

reduce its viscosity. This makes the liquid easy to be injected into the reactor system through a pump.

2.2. Catalyst preparation

Three catalysts were used for the combined upgrading of the bio-oil. The reforming catalyst was commercially available nickel-net. The hydrotreating catalyst was a multicomponent solid (Co–Ru–Zr/silica) with cobalt as the main catalyst and Ru and Zr as promoters. Porous silica was the catalyst support. The upgrading catalyst was Pt-ZSM-5, prepared from ammonium type ZSM-5 (Si/Al = 30) provided by Alfa Aesar. Pt species were introduced by wet impregnation and calcination in air.

Preparation of Co–Ru–Zr/silica: to 150 ml deionized water were added $Co(NO_3)_2{\cdot}6H_2O$ (9.88 g), $RuCl_3{\cdot}3H_2O$ (0.139 g) and $Zr(NO_3)_4{\cdot}5H_2O$ (4.71 g). The solution was heated to 90 °C and fumed silica (10 g, 500 m^2/g from Alfa Aesar) was added under careful stirring. The mixture was further heated to remove water under stirring. The dry solids were first calcined in air at 350 °C for 2 h and further treated at 550 °C for 3 h. The catalyst was activated by flow of H_2/Ar (10%) at 400 °C in the reactor before using. The elemental composition of the catalyst is Co (20 wt%), Ru (0.5 wt%) and Zr (10 wt%).

Preparation of Pt-ZSM-5: 22.8 mg of ammonium hexachloroplatinate (IV) (99%, CAS: 16919-58-7, from Strem) was dissolved in 3 ml of deionized water. 1.0 g of ammonium type ZSM-5 (Alfa Aesar 45880, Si/Al: 30/1) was added into the solution and the mixture was gently heated to remove water. The impregnated ZSM-5 was further calcined in air 550 °C for 3 h. The catalyst was activated by flow of H_2/Ar (10%) at 400 °C in the reactor before using. The metal load of Pt is 1.0 wt%. Ammonium type ZSM-5 was transformed to H-ZSM-5 through the calcination treatment.

2.3. Setup of the combined catalytic upgrading process

The combined catalytic upgrading process consists of two separate reactors: the reforming reactor and the upgrading reactor, as shown in Scheme 1. A model testing equipment was set up in our laboratory (Fig. S2). The reforming reactor is a high-temperature stainless steel tube (310 s, Ø30 mm outer diameter, 5 mm wall thickness). Five layers of nickel net (200 mesh) were fixed in the reactor by inert ceramic rings. Reforming temperature is 420 °C. The mixture of bio-oil/methanol is pumped into the reactor with the feed rate of 3.0 ml/h. WHSV in the reforming reactor is 1.53 h^{-1}. The flow from the reforming reactor is led into the upgrading reactor through a preheating pipe (450 °C). The upgrading reactor is a high-temperature stainless steel tube (310 s, Ø30 mm outer diameter, 5 mm wall thickness). Co–Ru–Zr/silica (0.12 g) and Pt-ZSM-5 (0.1 g) were mixed and diluted with inert SiC particles (0.16 g, 100 mesh). The solid mixture was packed in the reactor. The dead volume was filled with the quartz wool. Upgrading temperature was 450 °C. No carrier gas was introduced into the system and the reaction flow is generated in the reforming reactor (0.1–0.6 MPa). The hot outlet from the reaction system was led into a condenser with ice water. Liquid products were collected and gaseous mixture was sampled and released.

2.4. Materials characterization and products analysis methods

XPS data of the fresh and spent catalysts were obtained with an ESCALab220i-XL electron spectrometer from VG Scientific using 300 W Al Kα radiation. The base pressure was about approximately 3×10^{-9} mbar. The binding energies were referenced to the C 1s line at 284.8 eV from adventitious carbon. The Eclipse V2.1 data analysis software supplied by the VG ESCA-Lab200I-XL instrument manufacturer was used to manipulation of the acquired spectra. Nitrogen-adsorption isothermal and textural properties of the as-synthesized materials were determined by using liquid nitrogen over a Quantachrome Autosorb Automated Gas Sorption System (Quantachrome Corporation). Scanning electron microscopy (SEM) was conducted on an Fei XL 30 ESEM-FEG. The accelerating voltage for SEM studies was 15 kV. Specimens for SEM studies were prepared by dispersing materials in acetone by ultrasonic treatment and dropping the mixture onto SEM sample slides. Transmission electron microscopy (TEM) was performed by a JEOL 2010 TEM operated with an accelerating voltage of 200 kV. Powder X-ray diffraction (XRD) patterns were measured on a Rigakdu Rotaflex diffractometer equipped with a rotating anode and a Cu Kα radiation source (40 kV, 200 mA; λ = 1.54056 Å). NH_3-TPD and H_2-TPR were performed over an automated chemisorption analyzer (AutoChemII 2920, Micromeritics).

After the reaction, the gas outlet was analyzed by using a GC-2014 (Shimadzu) equipped with a packed column and a TCD detector. Liquid products were analyzed by GC and GC–MS. GC was performed on a GC-2014 (Shimadzu) equipped with a high-temperature capillary column (MXT-1, 30 m, 0.25 mm ID) and an FID detector. GC–MS was performed over on a GCT Premier/Waters instrument equipped with a capillary column (DB-5MS/J&W Scientific, 30 m, 0.25 mm ID).

2.5. Parameter calculations

$$\text{Carbon balance}: \quad \frac{G+L+C-M}{B} = 100\%.$$

where G is the number of moles of carbon in the gas release after the reaction, L the number of moles of carbon in liquid products after the reaction, C the number of moles of carbon in coke after the reaction, M the number of moles of carbon in added methanol after the reaction and B the number of moles of carbon in bio-oil feedstocks.

$$\text{Liquid product carbon yield}: \quad Y = \left(\frac{L}{B}\right) \times S \times 100\%$$

where S (selectivity) $= (N_i \times S_i)/(N_1 \times S_1 + \ldots + N_m \times S_m) \times 100\%$, N_i the carbon number of the detected molecule and S_i the GC–MS determined percent of the detected molecule.

3. Results and discussion

3.1. Reforming generation of hydrogen for hydrotreating

In our experimental operation, the reforming reactor has two functions: reforming of oxygenates and gasification of heavy components of bio-oil. Commercially available nickel net is selected as the structured catalyst for reforming with short contact time and the heating grid for gasification.

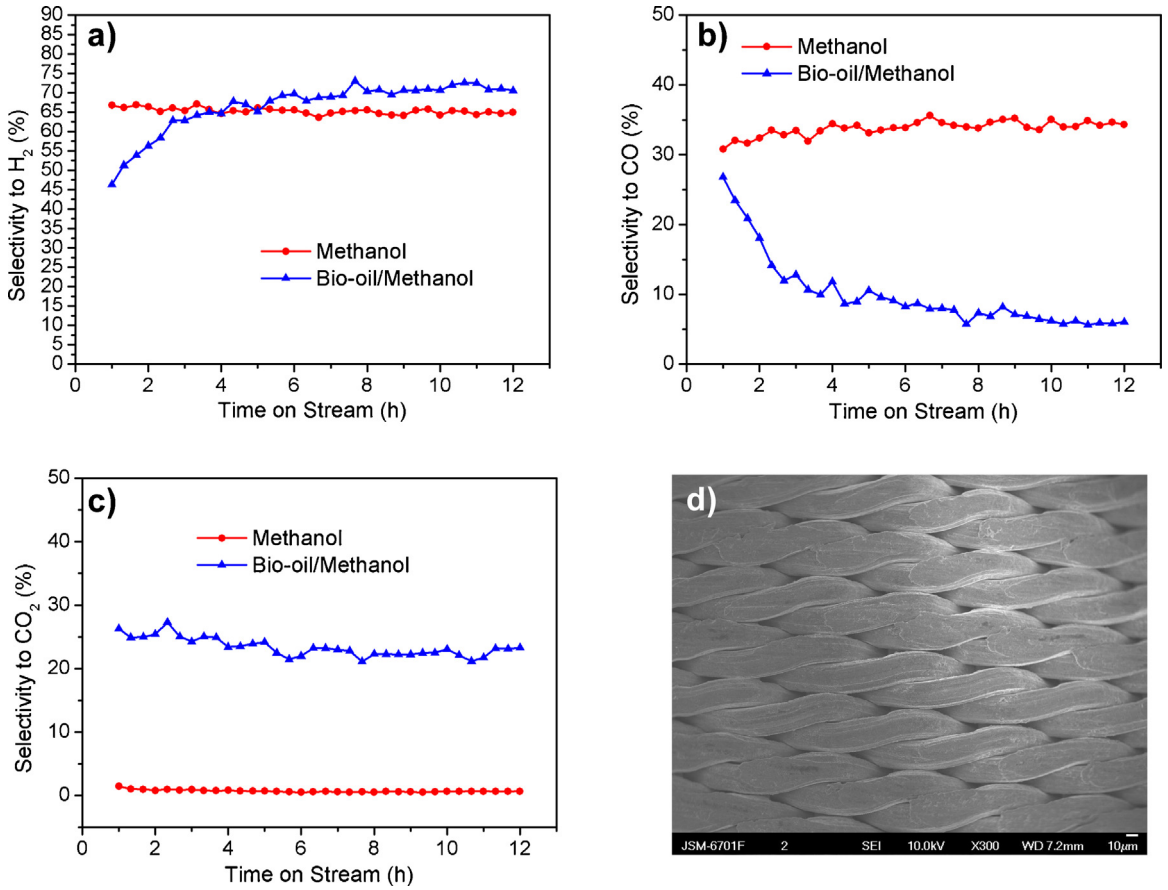

Fig. 1. (a) Hydrogen selectivity in the gas after reforming step. (b) CO selectivity in the gas after reforming step. (c) CO_2 selectivity in the gas after reforming step. (d) SEM image of the spent nickel-net catalyst.

Bio-oil was introduced into the reaction system. There was high content of water in the reaction flow. Hydrogen was produced from methanol and oxygenates mainly by steam reforming. Anhydrous methanol was injected into the reforming reactor under typical reaction conditions. Methanol was directly decomposed into hydrogen and carbon monoxide (Fig. 1a and b). The one-pass conversion of methanol is above 99%. Bio-oil/methanol mixture (methanol, 16 wt%) produced hydrogen-enriched gas mixture (its average composition: 71% hydrogen, 23% CO_2 and 6% CO) (Fig. 1a). Carbon element of methanol and oxygenates was mainly released as carbon dioxide by steam reforming (Fig. 1c). Water contents in the bio-oil cause water-gas-shift (WGS) reaction that is favored over nickel catalyst at the reforming temperature. Carbon monoxide is converted into carbon dioxide and hydrogen. However, WGS is a reversible reaction and carbon monoxide is not totally consumed (Fig. 1b). WGS directly leads to sharp decrease in the selectivity of carbon monoxide. The formation of carbon dioxide during reforming of bio-oil/methanol mixture is a more complex process that includes WGS and direct decomposition of methanol and oxygenates. Carbon element of methanol and oxygenates was mainly released as carbon dioxide by steam reforming (Fig. 1c). After the reforming step, liquid mixtures were collected. Methanol was totally converted and the composition of bio-oil was significantly modified. As shown in Table 2, organic acid and esters were not detected after the reforming step. These oxygenates were consumed in steam reforming for hydrogen generation. Nickel nets were used as reforming catalyst and heating grid for gasification. The spent nickel net was examined by SEM. The metal surface was clean (Fig. 1d). In our experimental observation, the performance of the reforming reactor was kept constant during 24-h testing.

3.2. Upgrading of bio-oil in the combined catalytic reactor

As shown in Scheme 1, upgrading of reaction flow from the reforming unit proceeds in a fixed-bed reactor, in which two solid catalysts are loaded in a physically mixing model. To avoid the high pressure drop during reaction, SiC particles (100 mesh) are used to dilute the catalyst bed. Table 3 lists the experimental results of four typical processes. Direct processing of YMB-BO over Ni-net cause steam reforming of some lightweight oxygenates and the corresponding carbon elements are rejected as carbon dioxide (entry 1 in Table 3, 21.7%). Reaction of YMB-BO over the combined upgrading catalysts results in heavy coke deposition over the catalyst layers (entry 2 in Table 3, 59.1%). If the bio-oil feedstock is

Table 2
Comparison of chemical components of bio-oil after the reforming step with the fresh sample.

Compound types	YMB-BO (relative area, %)	After reforming (relative area, %)
Aromatics	1.46	2.37
Organic acids	15.55	–
Furans	8.7	7.52
Ketones	14.17	8.43
Light phenols	12.36	24.7
Heavy phenols	13.23	18.5
Anhydrosugar	3.53	–
Total	69	54

Reaction conditions: Reforming was performed over nickel-net in a high-temperature stainless steel tube (310 s, Ø30 mm outer diameter, 5 mm wall thickness). Reforming temperature is 420 °C. The mixture of bio-oil/methanol is pumped into the reactor with the feed rate of 3.0 ml/h.

Table 3
Carbon yields of gas phase and liquid products after upgrading bio-oils through the combined catalytic process.

Entry	Feed	Reaction process	Carbon yield of gas phase and liquid products (%)					
			CH_4 or light hydrocarbon	CO_x	Aromatics	Alkanes/olefins	Coke	Others
1	YMB-BO	Ni-net	0	21.7	0	0	7.8	70.5
2	YMB-BO	Combined catalysts	0	13.4	8.5	6.7	59.1	12.3
3	YMB-BO	Ni-net + combined catalysts	3.1	23.5	16.1	7.2	39.2	11.9
4	YMB-BO + MeOH	Ni-net + combined catalysts	5.5	20.8	53.7	7.5	7.1	5.4

Reaction conditions: Reforming was performed over nickel-net in a high-temperature stainless steel tube (310 s, Ø30 mm outer diameter, 5 mm wall thickness). Reforming temperature is 420 °C. The mixture of bio-oil/methanol is pumped into the reactor with the feed rate of 3.0 ml/h. The flow from the reforming reactor is led into the upgrading reactor through a preheating pipe (450 °C). Co–Ru–Zr/silica (0.12 g) and Pt-ZSM-5 (0.1 g) were mixed and diluted with inert SiC particles (0.16 g, 100 mesh) in the upgrading reactor. The dead volume was filled with the quartz wool. Upgrading temperature was 450 °C.

pretreated over the nickel catalyst, the coke formation is markedly suppressed (entry 3 in Table 3, 39.2%) and the carbon yield of aromatics increases to 16.1%. The addition of methanol into the feedstock significantly improves the quality of upgrading products (entry 4 in Table 3). Carbon sources from methanol are excluded in the calculation of product carbon yields of bio-oil. The carbon yield of aromatics reaches 53.7%. The coking carbon decreases to 7.1% (after 24 on the reaction stream). The total yield of hydrocarbons is above 65%.

The composition of liquid products (from the process of entry 4 in Table 3) was analyzed by GC–MS. Approximately 20 types of aromatic compounds can be identified (Fig. 2). Their structural formulas are listed as the insets of Fig. 2. The structural information is derived from the detailed MS spectra (in Supporting Information). Some enriched compounds are benzene derivatives, such as **1** toluene, **3** PX, **7** trimethylbenzene and **16** naphthalene, which are among the most widespread and important chemical raw materials for synthetic plastics and fiber [35]. The aromatic mixtures are highly compatible with conventional hydrocarbon fuels and can be used as fuel additives. Jet fuel generally contains 15–25 vol.% of aromatics [36]. The upgrading products of bio-oil are potentially aromatic additives of jet fuels.

The carbon yield of aromatics is 16.1%, when bio-oil is directly processed through the reforming and upgrading reactors. Most of the components are deposited as coke (39.2%). The composition of aromatic products is more complicated and has relatively high oxygen content. As shown in Fig. 3, there are many phenolic compounds in the product mixture. Under the poor-hydrogen condition, the yield of aromatics is poor and hydrodeoxygenation is incomplete.

3.3. Correlation between physicochemical properties of the catalysts and their performance

Reaction flow from the reforming reactor is further upgraded over several types of solid catalysts (Table 4). Reaction over H-ZSM-5 results in heavy coke and the carbon yield of aromatics is 15.7%. When Pt nanoparticles are introduced into ZSM-5 (Pt load: 1.0 wt%), the aromatic yield increases markedly to 33.4%, however, coke deposition is very high. The presence of hydrotreating catalyst can suppress the formation of coke. Cobalt supported over silica is the main catalyst. Introducing Zr and Ru as the catalytic promoters can keep coke deposition at a low level (10.2%). The combination of Co–Ru–Zr/silica with Pt-ZSM-5 in the upgrading reactor gives the highest yield of aromatics (53.7%). The mixing model of the two catalysts also significantly affects the upgrading performance. When hydrotreating catalyst and zeolite catalyst are fixed in separate layers in a single reactor, the aromatic yield decreases to 39.3%.

Hydrotreating catalyst is a multicomponent solid supported over porous silica. All chemical elements, including Co, Ru, Zr and Si, are measured by XPS survey spectrum (Fig. 4a). Their microstructures are characterized by TEM (Scheme 1) and catalytic particles over silica can clearly discriminated from the background. The experimental results reveal that Ru and Zr are efficient catalytic promoters for cobalt to suppress coke deposition and increase

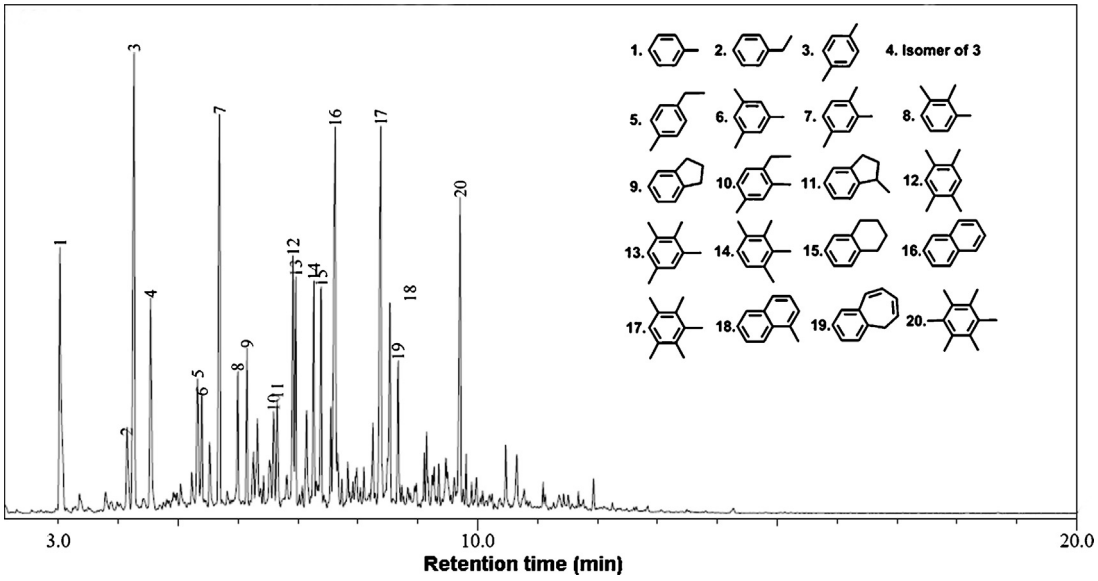

Fig. 2. GC spectrum of liquid products of entry 4 in Table 3.

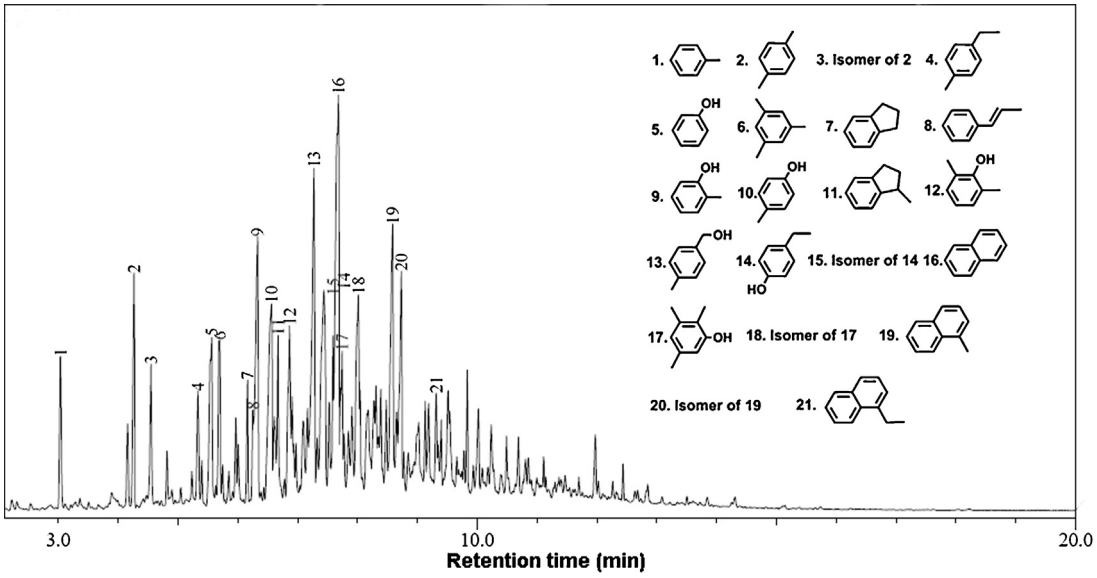

Fig. 3. GC spectrum of liquid products of entry 3 in Table 3.

the carbon yield of aromatics (entries 3–5 in Table 4). Fig. 5a shows the powder XRD patterns of three unreduced samples: A (Co–Ru–Zr/silica), B (Co–Zr/silica) and C (Co/silica). The broad bands from 20° to 30° are attributed to amorphous silica. The sharp peaks are indexed to cobalt oxide phases (C pattern). The addition of Zr leads to the identification of a weak peak overlapped by silica band. The Ru load is very low (0.5 wt%) and powder XRD pattern shows no marked change caused with its addition. After being reduced by hydrogen flow, all powder XRD patterns show significant changes (Fig. 5b). The peak intensity of cobalt oxide species sharply decreases. With the addition of Zr and Ru, the typical peaks of cobalt oxide species gradually disappear from XRD patterns. It is revealed that Zr and Ru species can promote the reduction degree of cobalt oxides.

Fitting of the Co 2p envelopes resulted in the identification of two chemical states of cobalt: one with a binding energy of 778.7 eV

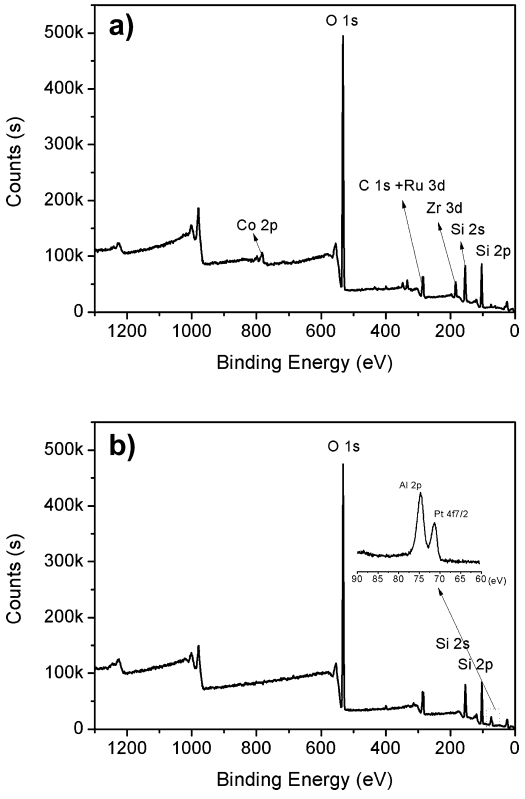

Fig. 4. (a) XPS survey spectrum of Co–Ru–Zr/silica. (b) XPS survey spectrum of Pt-ZSM-5.

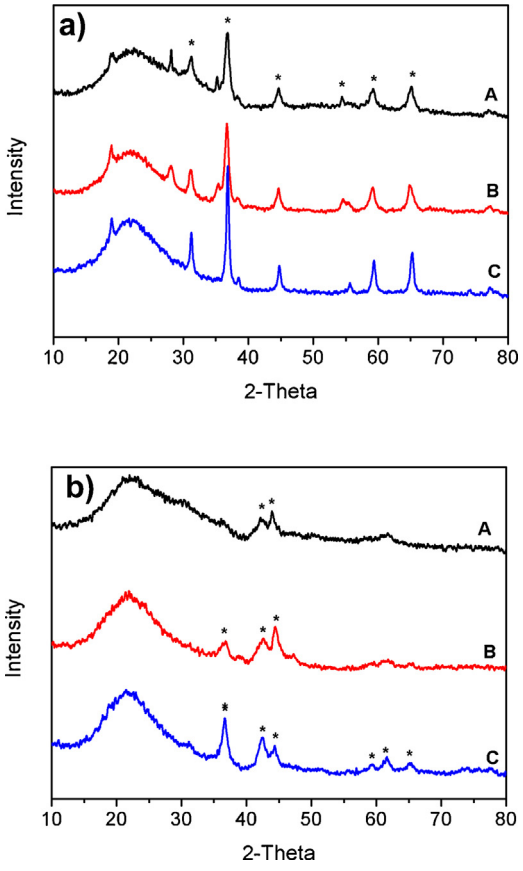

Fig. 5. (a) Powder XRD patterns of three calcined catalysts: (A) Co–Ru–Zr/silica; (B) Co–Zr/silica; (C) Co/silica. (b) Powder XRD patterns of the catalysts reduced by a hydrogen flow.

Table 4
Screening experiments over various upgrading catalysts.

Entry	Upgrading catalysts	Carbon yield of gas phase and liquid products (%)					
		CH_4 or light hydrocarbon	CO_x	Aromatics	Alkanes/olefins	Coke	Others
1	H-ZSM-5	0	24.4	15.7	7.2	39.3	13.4
2	Pt-ZSM-5	0	23.2	33.4	8.2	28.8	6.4
3	Co/silica	2.4	22.3	14.4	9.1	25.6	26.2
4	Co–Zr/silica	4.2	21.4	23.7	8.9	16.5	25.3
5	Co–Ru–Zr/silica	3.8	21.5	32.6	9.4	10.2	21.5
6	Co–Ru–Zr/silica + Pt-ZSM-5	5.5	20.8	53.7	7.5	7.1	5.4
7	Co–Ru–Zr/silica + Pt-ZSM-5 (layer-packed)	5.1	21.0	39.3	10.4	11.8	12.4

and another at 783.3 eV (Fig. 6). The Co $2p_{3/2}$ XPS peak at 778.7 eV is attributed to zero-valent cobalt and the signal at 783.3 eV can be indexed to cobalt oxide species. The atomic concentration of unreduced cobalt species is 45% for Co/silica. With the addition of Zr (10 wt%), the value decreases to 37%. The presence of Ru (0.5 wt%) reduces the proportion to 22%. This trend confirms the information provided by XRD patterns of the three samples (Fig. 5b). It is clear that the catalyst with the higher reduction degree is more active in hydrotreating process and more efficient in suppressing coke formation, as shown in entries 3–5 of Table 4.

The role of zirconium is different from that of ruthenium. H_2-TPR reveals that ruthenium with the load of 0.5 wt% significantly lowers the reduction temperature of supported cobalt species. The reduction of cobalt oxides begins at around 600 K and continues to nearly 1200 K (**1** in Fig. 7a). There is an expanded band of TCD signals that are attributed to water from reduction reaction with hydrogen flow. The direct reduction of Co/silica with hydrogen is difficult in achieving the high reduction degree of cobalt oxide species. However, the main reduction of Co–Ru/silica is completed before the temperature increase to 700 K (**2** in Fig. 7a). The role of ruthenium is to catalyze the reduction of cobalt oxides and guarantee relatively high surface concentration of catalytic active sites after hydrogen activation. Zirconia modifies the surface chemical properties of silica support. NH_3-TPD was used to investigate the surface acidity of two typical samples: (**2**, Co–Zr/silica) and (**1**, Co/silica) (Fig. 7b). All of the samples were treated under flowing argon at 773 K for 1.0 h to remove adsorbed organic pollutants. Adsorption of NH_3 was performed at 373 K in the NH_3/Ar flow (V/V: 10%) for 45 min. Desorption of NH_3 was conducted from 323 to 1173 K with the temperature increased at a rate of 2 K/min. The presence of zirconia introduces strong acidic sites onto the silica surfaces, which result in the strong peak at nearly 600 K. These acidic sites can markedly promote hydrodeoxygenation.

Platinum nanoparticles over ZSM-5 are kept in a monodispersed state and their average size is approximately 10 nm (Scheme 1).

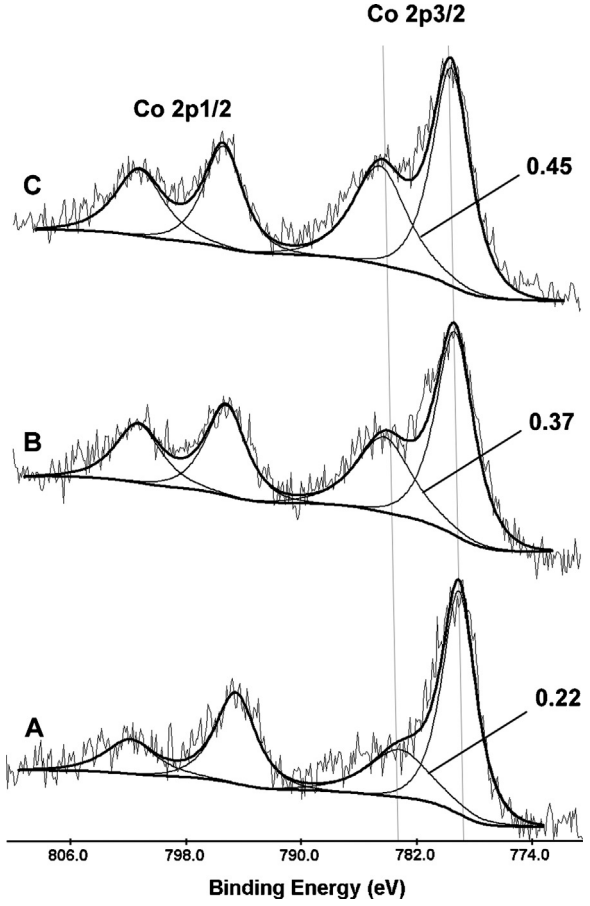

Fig. 6. XPS Co 2p peaks of the reduced catalysts: (A) Co–Ru–Zr/silica; (B) Co–Zr/silica; (C) Co/silica.

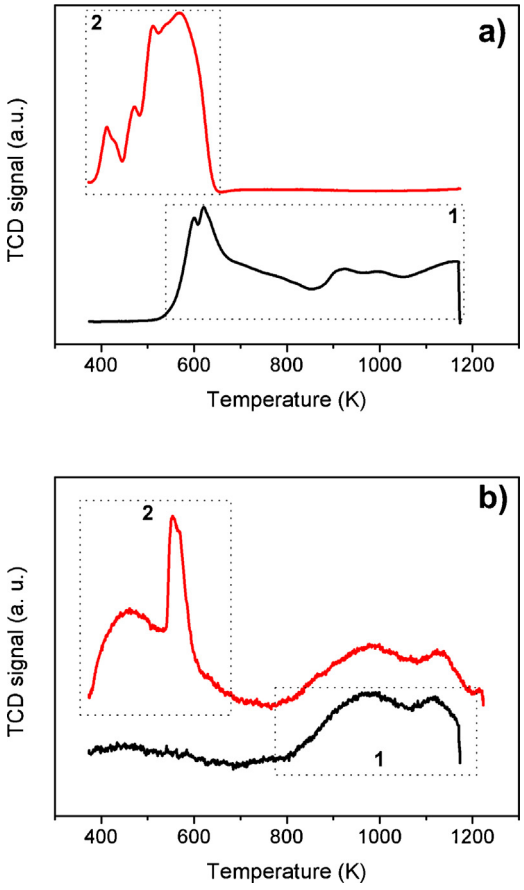

Fig. 7. (a) H_2-TPR measurement of Co/silica (**1**) and Co–Ru/silica (**2**). (b) NH_3-TPD measurement of the surface acidity of Co/silica (**1**) and Co–Zr/silica (**2**).

The presence of Pt nanoparticles significantly increases the carbon yield of aromatics through zeolite cracking process (entries 1–2 in Table 4); however, coke deposition is very high. Hydrotreating over Co–Ru–Zr/silica can suppress the coke formation. The combination of Co–Ru–Zr/silica with Pt-ZSM-5 in the upgrading reactor gives the highest yield of aromatics (53.7%) and the lowest coke deposition (7.1%) (Table 4).

4. Conclusions

In summary, pyrolysis oil from rice husks was upgraded through an integrated catalytic process and the carbon yield of aromatics was over 50%. The conversion included two sequent steps: reforming and upgrading. The function of the reforming step is *in situ* generation of hydrogen from methanol and low-weight molecules in bio-oil. Structured nickel nets were used as both the reforming catalyst and the heating grid for gasifying high-boiling-point components of bio-oil. The proportion of added methanol was 16 wt% of total bio-oil (including water). Methanol was not only the added hydrogen donor, but also polar solvent for homogenizing bio-oil and reducing its viscosity. In the upgrading reactor, the hydrotreating catalyst Co–Ru–Zr/silica and zeolite catalyst Pt-ZSM-5 were packed through a physical-mixture model. Hydrogen for deoxygenation is generated from reforming of added methanol and low-weight molecules in bio-oil. The combination of Co–Ru–Zr/silica with Pt-ZSM-5 in the upgrading reactor gave the highest yield of aromatics (53.7%) and the lowest coke deposition (7.1%). The proneness to coking during general fixed-bed upgrading can be significantly suppressed through the combined catalytic process.

Acknowledgements

This work was financially supported by the National Natural Sciences Foundation of China (Nos. 21101161, 21174148, 21304101) and YMB New Energy Co.

Appendix A. Appendix A

Supporting Information including: YMB-bio-oil properties, catalyst testing equipment, product analysis details. Figs. S1 and S2, Table S1, Detailed MS associated with Figs. 2 and 3 GC spectrum.

References

[1] A.V. Bridgwater, Biomass Bioenergy 38 (2012) 68–94.
[2] R.C. Brown, Thermochemical Processing of Biomass: Conversion into Fuels, Chemicals and Powder, Wiley, UK, 2011, pp. 1–12.
[3] D. Mohan, C.U. Pittman, P.H. Steele, Energy Fuels 20 (2006) 848–889.
[4] T.A. Milne, F. Agblevor, M. Davis, S. Deutch, D.A. Johnson, in: A.V. Bridgwater (Ed.), Developments in Thermochemical Biomass Conversion, Blackie Academic & Professional, London, 1997, pp. 409–424.
[5] P.M. Mortensen, J.D. Grunwaldt, P.A. Jensen, K.G. Knudsen, A.D. Jensen, Appl. Catal. A 407 (2011) 1–19.
[6] K. Jacobson, K.C. Maheria, A.K. Dalai, Renew. Sustain. Energy Rev. 23 (2013) 91–106.
[7] S.A. Chattanathan, S. Adhikari, N. Abdoulmoumine, Renew. Sustain. Energy Rev. 16 (2012) 2366–2372.
[8] S. Czernik, A.V. Bridgwater, Energy Fuels 18 (2004) 590–598.
[9] J.P. Diebold, S. Czernik, Energy Fuels 11 (1997) 1081–1091.
[10] P. Baglioni, D. Chiaramonti, K. Gartner, H.P. Grimm, I. Soldaini, G. Tondi, Biomass Bioenergy 25 (2003) 85–99.
[11] D.C. Elliott, T.R. Hart, G.G. Neuenschwander, L.J. Rotness, A.H. Zacher, Environ. Prog. Sustain. Energy 28 (2009) 441–449.
[12] D.C. Elliott, T.R. Hart, G.G. Neuenschwander, L.J. Rotness, M.V. Olarte, A.H. Zacher, Y. Solantausta, Energy Fuels 26 (2012) 3891–3896.
[13] V.A. Yakovlev, S.A. Khromova, O.V. Sherstyuk, V.O. Dundich, D.Y. Ermakov, V.M. Novopashina, M.Y. Lebedev, O. Bulavchenko, V.N. Parmon, Catal. Today 144 (2009), 362- 336.
[14] C. Zhao, Y. Kou, A.A. Lemonidou, X. Li, J.A. Lercher, Angew. Chem. Int. Ed. 48 (2009) 3987–3990.
[15] J. Wildschut, F.H. Mahfud, R.H. Venderbosch, H.J. Heeres, Ind. Eng. Chem. Res. 48 (2009) 10324–10334.
[16] A.R. Ardiyantia, A. Gutierrezb, M.L. Honkelab, A.O.I. Krauseb, H.J. Heeresa, Appl. Catal. A 407 (2011) 56–66.
[17] M.V. Bykova, D.Yu. Ermakov, V.V. Kaichev, O.A. Bulavchenko, A.A. Saraev, M.Yu. Lebedev, V.A. Yakovlev, Appl. Catal. B 113–114 (2012) 296–307.
[18] A.G. Gayubo, A.T. Aguayo, A. Atutxa, R. Prieto, J. Bilbao, Energy Fuels 18 (2004) 1640–1647.
[19] B. Valle, A.G. Gayubo, A. Alonso, A.T. Aguayo, J. Bilbao, Appl. Catal. B 100 (2010) 318–327.
[20] B. Valle, A.G. Gayubo, A.T. Aguayo, M. Olazar, J. Bilbao, Energy Fuels 24 (2010) 2060–2070.
[21] C. Zhao, J.A. Lercher, Angew. Chem. Int. Ed. 51 (2012) 5935–5940.
[22] R. Trane, S. Dahl, M.S. Skjøth-Rasmussen, A.D. Jensen, Int. J. Hydrogen Energy 37 (2012) 6447–6472.
[23] F.H. Mahfud, I. Melian-Cabrera, R. Manurung, H.J. Heeres, Trans. IChemE B: Process Saf. Environ. Prot. 5 (B5) (2007) 466–472.
[24] J. Xu, J. Jiang, W. Dai, T. Zhang, Y. Xu, Energy Fuels 25 (2011) 1798–1801.
[25] S. Miao, B.H. Shanks, Appl. Catal. A 359 (2009) 113–120.
[26] J.R. Regalbuto, Science 325 (2009) 822–824.
[27] T.P. Vispute, H. Zhang, A. Sanna, R. Xiao, G.W. Huber, Science 330 (2010) 1222–1227.
[28] V. Subramani, P. Sharma, L. Zhang, K. Liu, in: K. Liu, C. Song, V. Subramani (Eds.), Hydrogen and Syngas Production and Purification Technologies, Wiley, New Jersey, 2010, pp. 14–112.
[29] L. Garcia, R. French, S. Czernik, E. Chornet, Appl. Catal. A 201 (2000) 225–239.
[30] M. Ni, D.Y.C. Leung, M.K.H. Leung, K. Sumathy, Fuel Process. Technol. 87 (2006) 461–472.
[31] J. Agrell, B. Lingstrom, L.J. Pettersson, S.G. Jaras, Catalysis 16 (2002) 67–127.
[32] L. Wang, D. Li, M. Koike, S. Koso, Y. Nakagawa, Y. Xu, K. Tomishige, Appl. Catal. A 392 (2011) 248–255.
[33] C. Wu, L. Wang, P.T. Williams, J. Shi, J. Huang, Appl. Catal. B 108–109 (2011) 6–13.
[34] F. Bimbela, D. Chen, J. Ruiza, L. Garcia, J. Arauzo, Appl. Catal. B 119–120 (2012) 1–12.
[35] H.J. Arpe, Industrial Organic Chemistry, 5th Ed., Wiley-VCH, Germany, 2010, pp. 321–343.
[36] T. Edwards, in: M.L. Witten, E. Zeiger, G.D. Ritchie (Eds.), Jet Fuel Toxicology, CRC Press, Boca Raton, 2011, pp. 21–26.